Apolipoprotein A-I localization and dipalmitoylphosphatidylcholine dynamics in reconstituted high density lipoproteins

ARTICLE *in* CHEMISTRY AND PHYSICS OF LIPIDS · FEBRUARY 2000

Impact Factor: 2.42 · DOI: 10.1016/S0009-3084(99)00125-5 · Source: PubMed

2 AUTHORS, INCLUDING:

Alexander D Dergunov
National Research Center for Prevent…

72 PUBLICATIONS **384** CITATIONS

SEE PROFILE

ELSEVIER

Chemistry and Physics of Lipids
104 (2000) 161–173

CPL
CHEMISTRY AND PHYSICS OF LIPIDS

www.elsevier.com/locate/chemphyslip

Apolipoprotein A-I localization and dipalmitoylphosphatidylcholine dynamics in reconstituted high density lipoproteins

Alexander D. Dergunov [a,*], Gennady E. Dobretsov [b]

[a] *National Research Centre for Preventive Medicine, 10, Petroverigsky Street, 101953 Moscow, Russian Federation*
[b] *Research Institute for Physical Chemical Medicine, 119828 Moscow, Russian Federation*

Received 19 May 1999; received in revised form 22 September 1999; accepted 4 October 1999

Abstract

The structure and molecular dynamics of recombinant high density lipoproteins (rHDL) were studied by non-radiative energy transfer (NRET), fluorescence anisotropy and intensity measurements. The rHDL particles contained human plasma apolipoprotein (apo) A-I and dipalmitoylphosphatidylcholine (DPPC). Fluorescent *cis*- and *trans*-parinaric acids were used both as probes of molecular motion in the particle lipid phase and as acceptors in the Forster's energy transfer from apo A-I tryptophan residues to determine particle dimensions, apolipoprotein localization and lipid dynamics. The probes are sensitive to thermal wobbling (macromobility) and conformational deformations (micromobility) of phospholipid acyl chains. The experimental data fitted to various models of the particle structure are compatible with the following: (a) at $T < T_t$ the particles appeared as lens-like discs with a radius of the lipid phase of 5 nm and a mean thickness of 4 nm, the value being more by 20% in the particle centre, the α-helices of about 1 nm thickness were located around the edge of the lipid core. Compared to liposomes, both macro- and micromobility of DPPC molecules in rHDL were more rapid due to a significant disorder of the boundary lipid molecules close to the apo A-I molecule. This disorder led to the increase of the specific surface area per one lipid molecule, S_o. The lipid phase can be divided into three regions: (i) zone I of the most tightly packed lipid (0–1.7 nm from the disc axis) with a S_o value small as 0.5 nm^2; (ii) intermediate zone II (from 1.7 to 4.0 nm); and (iii) boundary lipid zone III (4–5 nm) of significantly disordered lipid with a S_o value large as 0.65 nm^2. (b) at $T > T_t$ the S_o heterogeneity disappeared, the radius of the lipid phase did not increase significantly, not exceeding 5.2–5.4 nm, but protein-induced immobilization of lipid molecules which affected about half or more of the total lipid, became remarkable. The overall effect was the supression of the transition amplitude in rHDL compared to liposomes. The structural inhomogeneity might underlie the function of the native plasma HDL as the key component of the transport and metabolism of plasma lipids.

Abbreviations: apoA-I, apolipoprotein A-I; *cis*-PA, *cis*-parinaric acid; DPPC, dipalmitoylphosphatidylcholine; HDL, high density lipoproteins; NRET, non-radiative energy transfer; rHDL, reconstituted high density lipoproteins; *trans*-PA, *trans*-parinaric acid; T_t, phospholipid transition temperature.

* Corresponding author. Tel.: +7-95-927-0324; fax: +7-95-928-5063.
E-mail address: dergunov@img.ras.ru (A.D. Dergunov)

0009-3084/00/$ - see front matter
PII: S0009-3084(99)00125-5

Keywords: Apolipoprotein A-I; High density lipoproteins; Molecular dynamics; Non-radiative energy transfer; Protein–lipid interactions; Reconstituted HDL

1. Introduction

The conformation of the major HDL protein, apoA-I (Fielding and Fielding, 1995) and the charge of the particle (Jonas et al., 1985), as well as both these parameters (Sparks et al., 1992a,b) probably play a critical role in the regulation of HDL function and metabolism. The use of reconstituted particles consisiting of apolipoprotein, phospholipid and cholesterol proved useful in physico-chemical studies (Jonas, 1986; Dergunov et al., 1997). One of the most promising methods to study the molecular architecture of reconstituted HDL is the non-radiative energy transfer between the tryptophan residues of apoA-I used as donors and the fluorescent *cis*-parinaric acid and *trans*-parinaric acid, embedded in the lipid matrix, as energy acceptors. The NRET efficiency is a sensitive indicator of the distances between donor and acceptor groups and of the particle dimensions as well.

In a previous paper (Dobretsov et al., 1998) we studied the localization of apoA-I in rHDL by energy transfer experiments at 25°C, i.e. below the DPPC phase transition temperature (41°C). Based on the experimental data, the model was constructed as following: (1) the particles possess a discoidal structure with a disc radius of 6 nm and the thickness of 4 nm; (2) the central area of the particle with a radius of 5 nm is filled by phospholipid molecules; (3) the apolipoprotein shell with a thickness of 1 nm is located at the edge of the particle; (4) the apoA-I molecule does not insert into the lipid phase deeper than 0.2–0.3 nm; and (5) the probe molecules distribute into the different regions of the bilayer: *trans*-PA localizes at the central area with a radius of 4 nm while *cis*-PA is closer to the disc periphery, at radial distances from 2.8–5 nm. The existence of the partially disordered boundary lipid layer of 1–2 nm thickness in the close vicinity to apoA-I molecules was suggested.

In the present paper we studied the dimensions of these rHDL particles, the apoA-I localization and the lipid dynamics, i.e. different modes of lipid motions, in a wide temperature range by NRET and by fluorescence intensity and anisotropy measurements.

2. Materials and methods

2.1. Materials

Dipalmitoylphosphatidylcholine was purchased from Sigma (MO, USA). The *trans*- and *cis*-parinaric acids fluorescent probes were purchased from Molecular Probes (OR, USA) and stored at -20°C in an ethanol solution (about 0.5 mM) until use. Apolipoprotein A-I was isolated from delipidated human plasma high density lipoproteins by ion-exchange chromatography under denaturing conditions (Van Tornout et al., 1980). The purity of apolipoprotein was checked by SDS-PAGE (Laemmli, 1970) in a 8–25% acrylamide gradient (Pharmacia LKB Phast System). The apoA-I purity was greater than 95%.

2.2. Methods

The buffer used throughout this study was 50 mM Tris-HCl, pH 8.0; 0.15 M NaCl; 0.02% NaN_3.

2.2.1. The preparation and characterization of apoA-I/DPPC complexes

These procedures were described in details in our preceding paper (Dergunov et al., 1997). The initial DPPC/protein weight ratio was 3:1 and corresponded to a mole ratio of 115:1. Briefly, after cholate was removed from lipid/apoA-I/detergent mixture by incubation with Bio-Beads, complexes were reisolated by gel filtration on a Superose 6PG column and the Stokes diameters of the complexes (8.2 ± 0.2 nm, $n = 5$) were esti-

mated after calibration of the column. The efficiency of cholate removal was greater than 99.5% as estimated from a control experiment by inclusion of a tracer quantity of [^{3}H]-cholic acid into the initial mixture, i.e. complexes after Bio-Beads procedure contained less than 2 mol% cholate relative to DPPC content. The yield of complex formation was close to 100% as (1) neither free protein nor free lipid were detected in the elution profiles; and (2) the initial DPPC/protein ratio was retained in the complexes isolated (108:1). The chemical composition of the isolated complexes was assayed as follows: DPPC was measured by an enzymatic colorimetric assay (Biomerieux, France) and the apolipoprotein content was determined from absorbance value at 280 nm, using an extinction coefficient 11.5×10^2 $g^{-1}cm^2$ for apoA-I (Gwynne et al., 1974). Based on the complex stoichiometry, each complex is assumed to contain an average two molecules of apoA-I.

2.2.2. Liposome preparation

A volume of 5 mg aliquot of DPPC solution in chloroform was dried under nitrogen and under vacuum. 2 ml of buffer were added and the mixture was sonicated three times, 7 min, with a Branson sonifier equiped with a standard tip at 45°C under N_2, at a power of 55 W. The mixture was centrifuged in 900 μl aliquots for 15 min, at 100 000 rpm, 22°C in an Optima TLX ultracentrifuge (Beckman) with a TLA 120.2 fixed angle rotor. After centrifugation, the upper 775 μl from each tube were removed and 1.55 ml of the sample was loaded onto a Sepharose CL-4B column. The peak corresponding to single bilayer vesicles was collected and concentrated with Centricon 100 (Amicon).

2.2.3. Molar partition coefficients

These values for *cis*- and *trans*-PA partition between the lipid phase of either the liposomes or the lipid–apoprotein complexes and the aqueous phase were determined by absorption spectroscopy at 25 and 50°C as described by Sklar et al. (1979).

2.2.4. Theoretical calculations of NRET and its experimental determination

In a widely accepted model of the structure of apolipoprotein/phospholipid recombinants, these particles appear as discs the core of which consists of a phospholipid bilayer while the apolipoproteins are located at the edge of the disc (Brasseur et al., 1992; Jonas, 1992). For our purpose, these particles consist of three parts-lipid, donor and acceptor-which can overlap partially; the lipid part occupies the cylinder with the radius R and donor groups occupy the volume between the surfaces of two cylinders with the internal and external radii RD_{int} and RD_{ext}, respectively (Fig. 1). The tryptophan residues of apoA-I were as donor groups and lipid-embedded *cis*- or *trans*-PA were as acceptors. The temperature-dependent values of Forster radius R_o were calculated (Dobretsov et al., 1998) as 3.41 and 3.42 nm for *trans*-PA and 3.60 and 3.46 nm for *cis*-PA at 25 and 50°C, respectively.

Fluorescence measurements were done on an Aminco SPF-500 spectrofluorometer equipped with a polarizer accessory and interfaced to a computer. A 0.3×1.0 cm quartz cuvette was placed in the thermostated chamber with long side parallel to the excitation beam. The temperature was maintained with 0.1°C accuracy and was measured constantly with a thermocouple placed immediately above the excitation beam. Fluorescence of Trp residues was excited at 280 nm and area F under the emission curve at the range of 300–350 nm was considered to be proportional to

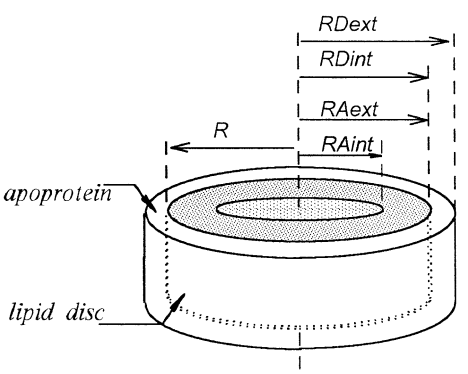

Fig. 1. Model of rHDL particle.

the fluorescence quantum yield Q. At the sequential probe addition to rHDL solution the F value decreased and a set of n experimental values Fe[0],… Fe[i],… Fe[n] was obtained which corresponded to the acceptor concentrations in a lipid-bound form Ca[0],… Ca[i],… Ca[n] (mol/l, Ca[0] = 0). The corresponding experimental errors were as Er[0],… Er[i],… Er[n]:

$$\mathrm{Er}[i] = \left[\frac{1}{k \cdot (k-1)} \cdot \sum_{j=1}^{j=k} (\mathrm{Fe}_j[i] - \mathrm{Fe}[i])^2 \right]^{1/2} \quad (1)$$

where Fe[i] is the mean value for a set of $\mathrm{Fe}_j[i]$ values from k separate experiments ($j = 1,\ldots k$) at the particular acceptor concentration Ca[i].

The set of calculated values of Fm[0],… Fm[i],… Fm[n] for the corresponding acceptor concentrations was obtained using the procedure outlined in the previous paper (Dobretsov et al., 1998) to fit NRET data to the molecular dimensions of rHDL within the model described above. To evaluate the accuracy of the fitting procedure, a least-squared criterion was used:

$$\chi^2 = \frac{1}{n} \cdot \sum_{i=1}^{i=n} \left[\frac{(\mathrm{Fm}[i] - \mathrm{Fe}[i])}{\mathrm{Er}[i]} \right]^2 \quad (2)$$

For the optimization routine to be valid, χ^2 value have to be smaller than one and any improvement of the model results in the decrease of χ^2 parameter.

2.2.5. Temperature-induced phase transition

To monitor temperature-induced phase transitions in the liposome and in the complexes, the sample in the cuvette (200 and 750 μM DPPC for complex and for liposome, respectively) with 4 μM *cis*- or *trans*-PA was placed into the cell chamber pre-heated to 55°C, and the temperature was gradually decreased to 25°C at a rate of 0.7° min^{-1} while measuring fluorescence anisotropy at fixed time intervals. For both probes, excitation was at 320 nm with 0.5 nm excitation slit, and emission was recorded at 420 nm with 10 nm slit. Total fluorescence F and anisotropy r values were calculated as

$$F = F_{\parallel} + 2F_{\perp} \quad (3)$$

$$r = \frac{F_{\parallel} - F_{\perp}}{F_{\parallel} + 2F_{\perp}} \quad (4)$$

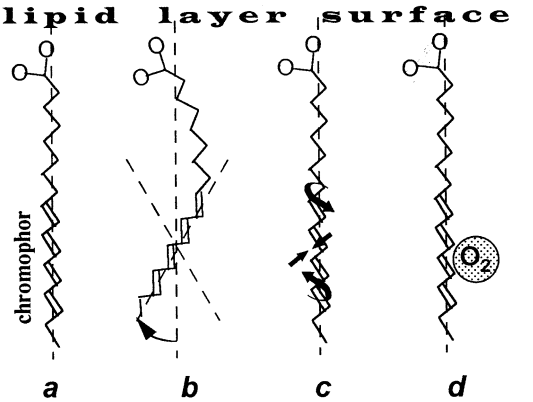

Fig. 2. Localization and different types of mobility of *trans*-PA in phospholipid bilayer. (**a**) probe chromophore location; (**b**) wobbling type motion of *trans*-PA chromophore; (**c**) chromophore deformations (rotations around and vibrations along the C–C bonds); (**d**) translational mobility of the probe molecules resulting in the fluorescence quenching by oxygen molecules. The normal to the lipid surface is depicted by the dotted line.

$F_{\parallel}$ and $F_{\perp}$ refer to parallel and perpendicular orientation of polarizer and analyzer, respectively. No correction for instrumental polarization was made as G-factor was nearly one (Lakowicz, 1983). With F and r parameters it is possible to make more precise conclusions about the probe microenvironment and its dynamics. The data were treated as the first order phase transition to obtain the transition parameters, i.e. the transition temperature T_t and the transition amplitude as the ratio of the probe fluorescence intensities F_s/F_f or anisotropies r_s/r_f at the transition midpoint extrapolated from low- and high-temperature regions, respectively ($\ll$s$\gg$-solid, $\ll$f$\gg$-fluid). Data were fitted by nonlinear least squares using the SAS package as described (Dergunov et al., 1997).

2.2.6. Lipid dynamics evaluation

The carboxy-group of parinaric acid has been assumed (Sklar, 1980) to localize at the lipid–water interface while fatty acid chain lies parallel to phospholipid acyl chain in the bilayer (Fig. 2a). The same localization of these probes was suggested in our preceding paper (Dobretsov et al., 1998). Three kinds of probe mobility are consid-

ered on the dimension scale comparable to the acyl chain diameter to evaluate semi-quantitatively the relations between measured r and F values and lipid dynamics: (1) the wobbling-type of the rotational mobility of the probe chromophore (Fig. 2b), referred below as 'macromobility'; (2) the deformations of separate segments of the chromophore, i.e. rotations around and vibrations along the C–C bonds (Fig. 2c), referred as 'micromobility'; and (3) the collisions between probe and oxygen molecules as a result of a translational mobility (Fig. 2d), with the amplitude intermediate between ones for the first two motion types.

(1) The macromobility contributes mainly to the anisotropy; the high r values were observed for immobilized probe molecules due to the parallel orientation of emission and absorption dipoles (Pfanstiel et al., 1989) while anisotropy was low in organic solutions and in fluid lipids (Sklar et al., 1977a,b). The thermotropic phase transitions in lipid bilayers were accompanied by the abrupt r decrease (Sklar et al., 1977b, 1979).

(2) The micromobility may determine the fluorescence quantum yield Q and intensity F values. The thermotropic phase transition may result in fluorescence quenching due to the increase of the frequency of vibrational and rotational motions along the chromophore axis (Christensen and Kohler, 1975, 1976; Birch and Birks, 1976; Birch and Imhof, 1982 Uphoff et al., 1989). The major effect of the transition on the Q and F values in our study may be proposed based on: (a) the high values of polyene quantum yield at low temperatures in liquid media and its continuous decline at heating (Birch and Imhof, 1982); (b) the similar monotonic decrease of quantum yield at heating within 25–50°C temperature range obtained for parinaric acids in lipids without the transition in this temperature region (Sklar et al., 1977a; Waring et al., 1979); and (c) the high Q values observed at room temperature for probes in the lipid gel phase (Sklar et al., 1977b; Waring et al., 1979).

(3) The possible contribution of lipid-dependent oxygen quenching to fluorescence quantum yield and intensity follows from (a) the existence of two-component decay curves for polyenes with characteristic times of three and 15–25 ns (Sklar et al., 1977a,b; Bel'kov et al., 1988); (b) the 2.4-times decrease of the long decay time at aeration of hydrocarbon solutions (Bel'kov et al., 1988); and (c) the abrupt decrease of the long-lived component after phospholipid phase transition (Sklar et al., 1977b).

Thus, both second and third types of the molecular motion seem to be responsible for Q and F changes at thermotropic transitions in rHDL.

To evaluate these effects on the fluorescence intensity in the case of the complex situation for polyenes (Christensen and Kohler, 1975, 1976; Birch and Birks, 1976; Sklar et al., 1977a; Waring et al., 1979; Birch and Imhof, 1982; Pfanstiel et al., 1989) the relation between Q and the rate constants of radiative (k_r) and radiationless (k_q) processes (Birch and Birks, 1976; Sklar et al., 1977a; Birch and Imhof, 1982) may be applied:

$$Q = \frac{k_r}{k_r + k_q} \tag{5}$$

It follows from Eq. (5) that quantum yield decreases at k_q increase which is sensitive to temperature-induced micromobility changes at the phase transition. To apply this relation to F value, the following assumptions were made: (1) the radiative rate constant k_r does not depend on the temperature within 25–50°C range that is typical for polyene chromophores Birch and Birks, 1976; Birch and Imhof, 1982; (2) the temperature-sensitive motion results in the change of k_q and, as a result, of Q values; (3) the intensity values are proportional to quantum yields for both probes based on the data of Sklar et al. (1977a,b) for parinaric acid probes in DPPC liposomes; and (4) for rHDL, the Q value outside the phase transition region is determined by single decay component with large and small decay times below and above the phospholipid transition temperature, respectively. Then the following equations are valid for decay time τ and k_r:

$$\tau(T) = \frac{1}{k_r + k_q(T)} \tag{6}$$

$$k_r = \frac{Q(T)}{\tau(T)} \tag{7}$$

Trans- and *cis*-PA in decane possess the Q values as 0.031 and 0.054 and τ values as 3.1×10^{-9} and 5.2×10^{-9} s, respectively (Sklar et al., 1977a); then calculated k_r values are 1.0×10^{7} s^{-1} for both probes which coincide with the experimental data for parinaric acids in hydrocarbon solvents (Sklar et al., 1977a). The following equation can be written by combination of Eqns. 6 and 7:

$$k_q = k_r \cdot \left(\frac{a}{F(T)} - 1 \right) \quad (8)$$

where a is a proportionality constant between Q and F parameters ($F(T) = a \cdot Q(T)$) derived from the known data (Sklar et al., 1977b) on quantum yield of the probes in DPPC liposomes outside the phospholipid transition region.

3. Results

3.1. Fluorescence anisotropy measurements

The representative data on temperature responses of fluorescence anisotropy of *trans*- and *cis*-PA in DPPC liposomes and in rHDL particles are given on Fig. 3 and the transition parameters from several experiments are summarized in Table 1. The following effects were observed for liposomes: (1) the r values at 25°C were high for both probes, i.e. at $T < T_t$ the macromobility is low; (2) DPPC phase transition resulted in the profound, two-fold decrease of fluorescence anisotropy of *cis*- and *trans*-PA at a narrow transition range with T_t values 40–41°C; (3) after the end of the

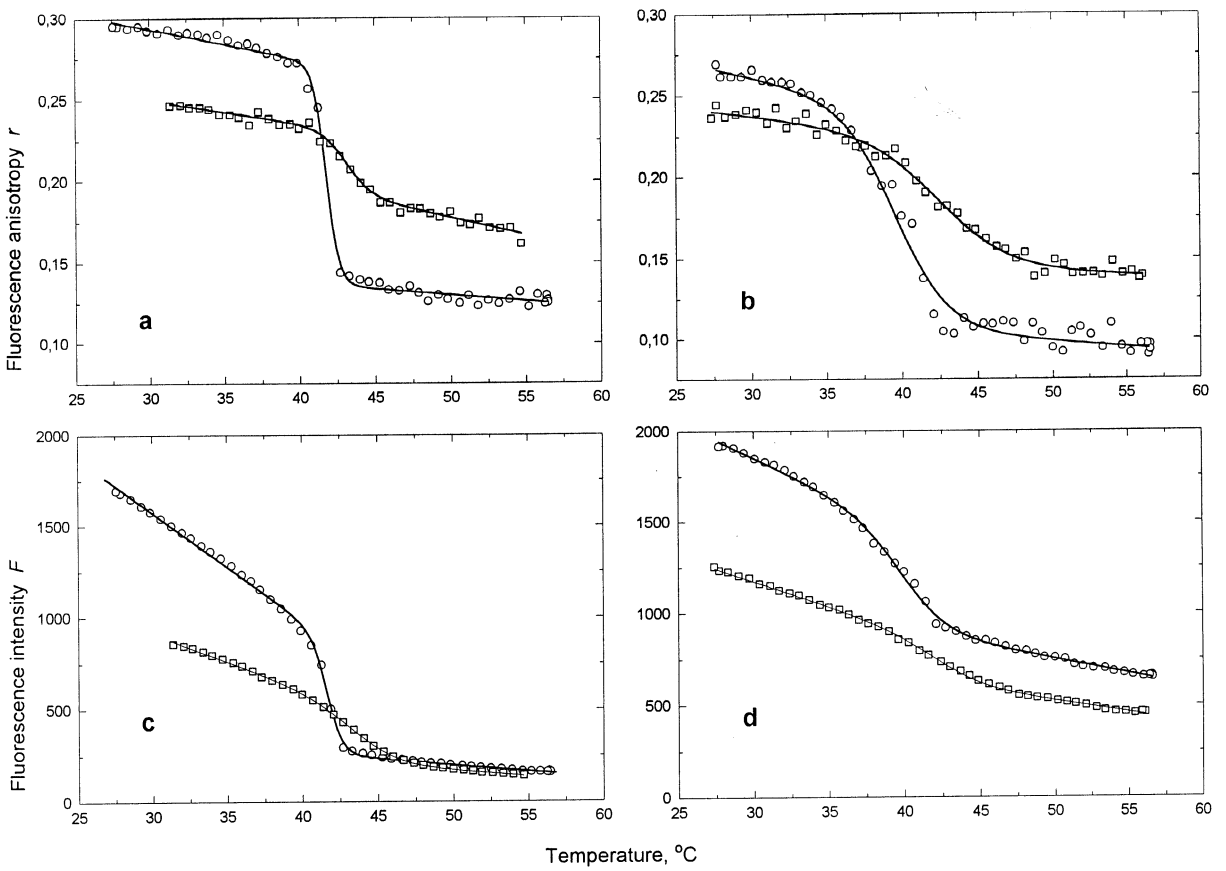

Fig. 3. The temperature dependence of fluorescence anisotropy r (**a**, **b**) and intensity F (**c**, **d**) of *trans*-PA (**a**, **c**) and *cis*-PA (**b**, **d**) in DPPC liposomes (circles) and in rHDL particles (squares). The lines between the experimental data points are the results of data fitting to the first order phase transition.

Table 1
The temperature-induced phase transition of DPPC in single bilayer liposomes and in reconstituted HDL[a]

	trans-PA		*cis*-PA	
	Liposomes (2)	rHDL (2)	Liposomes (5)	rHDL (2)
By fluorescence anisotropy				
T_t, °C	40.8 ± 0.3	44.7 ± 1.7	40.2 ± 0.2	42.3 ± 0.3
r_s/r_f	1.98 ± 0.01	1.19 ± 0.00	2.14 ± 0.04	1.51 ± 0.13
By fluorescence intensity				
T_t, °C	41.5 ± 0.2	46.4 ± 1.8	41.1 ± 0.3	43.2 ± 0.1
F_s/F_f	3.51 ± 0.08	2.66 ± 0.20	1.58 ± 0.06	1.42 ± 0.00

[a] The transition temperature T_t and the amplitude of the transition were measured by probe fluorescence intensity and anisotropy as descibed in Section 2. The values are given as mean $\pm$ SEM, the number of separate experiments are indicated in brackets.

transition there was no appreciable change of the rotational mobility of the probe molecules. These results agree with data of Sklar et al. (1979).

Compared to liposomes, the data for rHDL were as following: (1) below T_t, lower r values were obtained for both probes in spite of the different preferential localization of two isomers: *trans*-PA distributes into the central area of the particle while *cis*-PA segregates at the periphery of the particle (Dobretsov et al., 1998). Probably, at low temperatures the lipid phase of the particle compared to liposomes is characterized by an increased disorder that, in turn, may result in the increased rotational mobility of the probe molecules; (2) the transition shifted to higher temperatures by 2–4°C and its amplitude was lower than in liposomes, the latter was more evident for *trans*-PA compared to *cis*-PA and the ratios of the transition amplitudes in liposome versus rHDL were 1.7 and 1.4, respectively; and (3) after the phase transition, the r values for probe in rHDL compared to liposomes were significantly higher, probably due to the more restricted probe wobbling in the particles at $T > T_t$.

3.2. Fluorescence intensity measurements

The representative data on temperature responses of fluorescence intensity of *trans*- and *cis*-PA in DPPC liposomes and in rHDL particles are given on Fig. 3 and the transition parameters from several experiments are summarized in Table 1. The phase transition in liposomes observed at 41–41.5°C resulted in a mean intensity decrease of *trans*- and *cis*-PA of 3.5 and 1.6 times, respectively. Compared to liposomes, the data for rHDL were as following: (1) below T_t, the F values were lower for both probes, probably due to the increased segmental motion (micromobility) of chromophore group; (2) in analogy with the r measurements, the transition shifted to higher temperatures by 2–5°C and its amplitude was lower than in liposomes, especially for *trans*-PA compared to *cis*-PA and the ratios of the transition amplitudes in liposomes versus rHDL were 1.3 and 1.1, respectively; and (3) after the transition, the lipid micromobility in the particles and in rHDL depicted by the parameter F did not differ from each other, in contrast to the macromobility detected by r parameter.

The temperature dependency of the radiationless rate constant k_q for *cis*- and *trans*-PA in rHDL and in DPPC liposomes was calculated from the intensity measurements (Fig. 4). The effective characteristic time of the processes resulting in the intensity decrease and reciprocal to k_q value, was 30 ns for both probes in liposomes at $T < T_t$ and decreased after phase transition by 13 and 3.4 fold for *trans*- and *cis*-PA, respectively; perhaps, the increase of the molecular motion in the lipid environment of *trans*-PA is more pronounced compared to *cis*-PA. The k_q values at $T < T_t$ were two-fold higher for the probe incorporated in rHDL particles compared to liposomes and this difference disappeared at $T > T_t$, in agreement with the change of the parameter F at

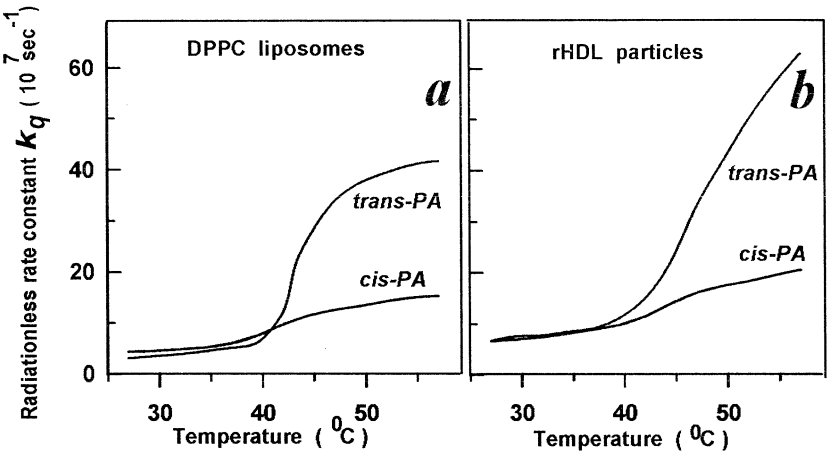

Fig. 4. The temperature dependence of the radiationless rate constant k_q for *trans*- and *cis*-PA in liposomes (**a**) and in rHDL particles (**b**). The k_q values were calculated from Equations 5–8.

the DPPC phase transition, implying a major contribution of the micromobility to the level of fluorescence intensity.

3.3. Trans- and cis-PA localization in rHDL

The problem was studied by NRET approach and the data for temperatures below and above T_t are presented on Fig. 5. The efficiency of energy transfer differed significantly for the two probes at 25°C as a consequence of the different localization of two parinaric acid isomers in the lipid phase of rHDL: *trans*-PA molecules occupy the central part of the disc while *cis*-PA accumulates on the disc periphery (Dobretsov et al., 1998). This difference disappeared at 50°C and the curves shifted to the same intermediate position, probably due to a random location of the probes molecules in the lipid phase, all the phase being accessible to probe molecules after the DPPC phase transition.

3.4. ApoA-I localization in rHDL

The phase transition in pure lipid bilayer results in the change of orientation of lipid molecules in bilayer with an increase of surface area and a proportional decrease of a bilayer thickness. After this transition the area per phospholipid molecule increases from 0.42 to 0.6–0.72 nm^2 (the values for fluid lipid measured by energy transfer between lipid-inserted probe molecules are close to 0.65 nm^2) (Levine, 1972; Phillips, 1972; Lapshin et al., 1983; Kurek et al., 1989). If the change of the surface area in rHDL is comparable to that in liposomes then the radius of the lipid phase R has to increase up to $(0.65/0.42)^{1/2} = 1.24$ times, i.e. from 5 to 6.2 nm. The R value coincided with the internal radius of the protein cylinder RD_{int} at $T < T_t$, i.e. $R = RD_{int}$ (Dobretsov et al., 1998); it

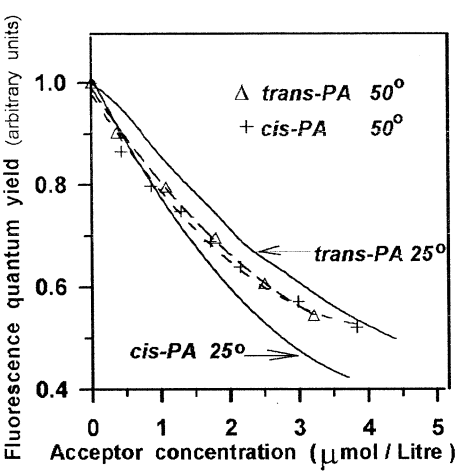

Fig. 5. The concentration dependence of the efficiency of energy transfer at 50°C (dotted lines). For comparison, data obtained at 25°C (solid lines) are also given (Dobretsov et al., (1998).

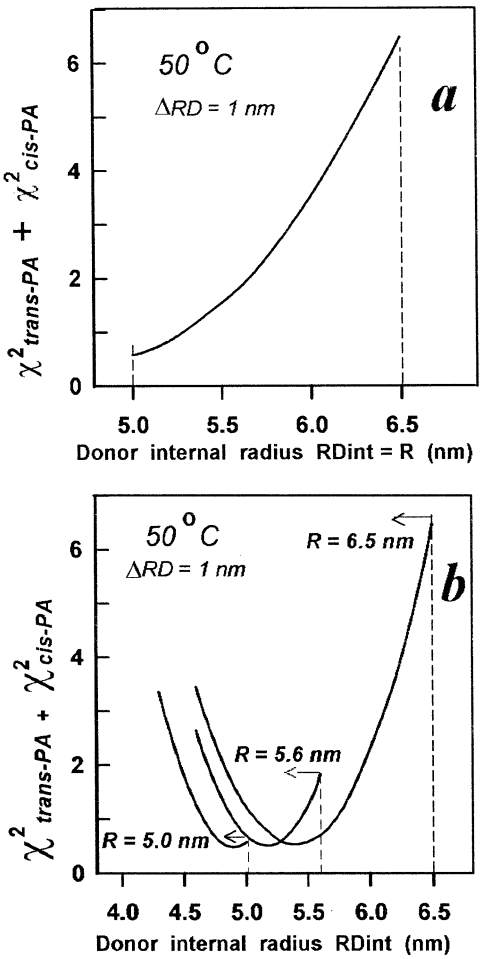

Fig. 6. Optimization of the particle dimensions at the random distribution of the probe molecules in the lipid phase and at the constant thickness of the protein layer as 1.0 nm. (**a**) the radius of the lipid phase R ($R = \mathrm{RD_{int}}$) was varied from 5.0 to 6.5 nm while keeping the lipid volume constant; the thickness of the lipid phase, fixed as 4.0 nm at $R = 5.0$ nm, decreased at the R increase. (**b**) the optimization of distance between the particle axis and the inner surface of protein cylinder $\mathrm{RD_{int}}$ at the three fixed values of R: 5.0, 5.6 and 6.5 nm ($R \neq \mathrm{RD_{int}}$). The sum of χ^2 values obtained for both probes is given.

seems to be reasonable to assume also the validity of this relation at $T > T_t$. The results of R evaluation obtained by fitting NRET data measured at 50°C, at varying $\mathrm{RD_{int}}$, are presented on Fig. 6a at $\mathrm{RD_{int}} = R$. Small χ^2 values, i.e. valid approximations were obtained only for the 5–5.4 nm range and the optimization efficiency failed at $\mathrm{RD_{int}}$ increase outside this range, i.e. no apolipoprotein molecule could be found at the periphery of the disc and only small increase of the lipid area size, from 5.0 to 5.2–5.4 nm, seems to be reasonable.

If the optimization routine was performed at $\mathrm{RD_{int}} \neq R$ (Fig. 6b), then optimal $\mathrm{RD_{int}}$ values within 4.9–5.0 nm range were obtained at $R = 5.0$ nm, i.e. the outer boundary of the lipid phase coincides with the inner surface of the apolipoprotein molecule, as at 25°C. At the increase of R parameter to a reasonable value of 5.6 nm and further to 6.5 nm, the distance between the particle axis and the inner surface of protein cylinder did not change significantly and the optimal $\mathrm{RD_{int}}$ values were 5.2 and 5.4 nm, respectively. These results suggest a partial immersion of apoA-I molecule into the lipid phase. Taking into account the thickness of the apolipoprotein shell expressed as $\Delta\mathrm{RD} = (\mathrm{RD_{ext}} - \mathrm{RD_{int}})$ which was fixed as 1.0 nm in the optimization routine, one can conclude about the absence of any appreciable changes of the distance between the particle axis and the centre of apolipoprotein molecule at the DPPC phase transition. This distance may vary only from (5.0 nm + (1/2)·1 nm) = 5.5 nm at 25°C to (5.4 nm + (1/2)·1 nm) = 5.9 nm at 50°C.

4. Discussion

4.1. Fluorescence anisotropy and intensity as indicators of phospholipid phase transition

The mobility of lipid molecules nearest to probe molecules influences both fluorescence intensity and anisotropy. Several types of molecular motion seem to contribute to the fluorescence parameters, i.e. anisotropy depends largely on the rotational mobility of the probe chromophore (Fig. 2b) referred as macromobility whereas the deformations of the individual segments inside the chromophore group (Fig. 2c) referred as micromobility and translational diffusion as well contribute to the fluorescence intensity. The main contribution of chromophore conformational deformations to F parameter seems to underly the analogous behaviour of experimentally measured intensity changes at DPPC phase transition (Fig.

3) and calculated profiles of non-radiative rate constants (Fig. 4) both in liposomes and rHDL. Thus, the combined use of the r and F parameters enabled to differentiate between the different kinds of probe molecular motions and to suggest the increase of both macromobility and micromobility in rHDL compared to liposomes at $T < T_t$; the partial disorder of the lipid part of the particles induced by apoA-I at low temperatures follows also from the absence of appreciable changes of the radial distance between the particle axis and protein molecule (Fig. 6) and from the different location of *trans*- and *cis*-PA at 25°C (Dobretsov et al., 1998). Three reasons may underly the differences observed between the pure lipid bilayer and the lipid phase of rHDL: (1) the small dimensions of the latter that may decrease the transition cooperativity; (2) the protein/lipid/water interface may induce the structural defect in the lipid packing; and (3) the apolipoprotein molecule may act as an impurity in the lipid lattice at gel state.

The F and r parameters decreased both upon thermotropic phase transition in rHDL particle, however, differences were observed at $T > T_t$: r values were higher for rHDL particles compared to liposomes while F values did not differ. Different from the same segmental motions of the probe in liposomes and in rHDL particles at $T > T_t$, the rotational mobility of *trans*- and *cis*-PA in rHDL decreased compared to liposomes, probably due to the immobilizing action of apoA-I molecule.

4.2. Boundary lipid hypothesis

The presence of a specific lipid layer(s) in the close vicinity to protein molecule is characterized by the following features.

(1) The absence of the appreciable changes of phospholipid transition temperature in protein/lipid recombinants compared to pure phospholipid bilayer either for hydrophobic protein–lipid interactions (Papahadjopoulos et al., 1975) or for the value of the order parameter of boundary lipid intermediate between that for gel and liquid–crystalline phases (Owicki and McConnell, 1979).

(2) The decrease of transition enthalpy observed by Tall and Lange (1978) for apoA-I/DMPC recombinants that may indicate the exclusion of the boundary lipid from the phase transition (Tall and Lange, 1978; Owicki and McConnell, 1979; Jonas and Matz, 1982). However, the existence of two broad and narrow components observed by differential scanning calorimetry for reconstituted systems from model hydrophobic peptide Lys_2-Gly-Leu_{24}-Lys_2-Ala-amide and homologous saturated phosphatidylcholines (Zhang et al., 1992) may originate from the melting of boundary lipid with smaller cooperativity. The data of Kimelman et al. (1979) seem to favor this conclusion: based on the phase transition study of DMPC in M13 coat protein/DMPC recombinants with the aid of parinaric acid probes, these authors suggested the decreased responce of fluorescence intensity of *cis*-PA to thermotropic phase transition.

(3) The varying action of protein molecule on the order paramater of phospholipid molecules both below and above T_t. The protein-induced decrease of the order parameter at $T < T_t$ was registered by Fourier transform infrared spectroscopy (Zhang et al., 1992) while the others observed the absence of mobility change (Kimelman et al., 1979; Zhang et al., 1992) or its decrease (Owicki and McConnell, 1979; Zhang et al., 1992) at $T > T_t$.

(4) The separation of protein and lipid regions (Owicki and McConnell, 1979; Zhang et al., 1992) as an extreme case of dismatch between the hydrophobic regions of protein and lipid. According to our data for apoA-I/DPPC complexes, the first three features from four mentioned are present. The decreased rotational mobility and homogeneous probe distribution in the whole lipid volume at $T > T_t$ are suggested to originate from the action of apoA-I as an additional impurity on the lipid packing as mentioned above already.

4.3. The change of rHDL dimensions at phase transition

The phospholipid phase transition in the bilayer from the synthetic phosphatidylcholines is accompanied by the change of orientation of phospho-

lipid acyl chains (Zhang et al., 1992) with the corresponding increase of the surface area. At the same time the NRET data (Fig. 5) about the absence of the appreciable changes of the radial dimension of rHDL particle at the DPPC phase transition suggest the absence of the appreciable changes of the DPPC surface area. The direct comparison of the surface area change in liposomes versus rHDL may be done by the measurements of the lipid surface area by the NRET approach (Lapshin et al., 1983; Kurek et al., 1989). However, the crude limit estimations can be done as follows. The number of DPPC molecules in the particle is $N_L = 2(\pi R^2/S_o)$, S_o is the surface area occupied by one DPPC molecule; at temperatures below and above T_t this parameter for pure lipid bilayer is taken as 0.42 and 0.65 nm^2, respectively (Levine, 1972; Phillips, 1972; Lapshin et al., 1983; Dobretsov et al., 1989; Kurek et al., 1989). Hence, the N_L value is equal to 374 at $T < T_t$ and, taking into the consideration the known DPPC/apoA-I molar ratio as 108:1 (Dergunov et al., 1997), the number of protein molecules per particle N_P can be calculated as $N_P = N_L/(N_L/N_P) = 374/108 = 3.5$. This value exceeds considerably the experimentally determined value close to 2 (Dergunov et al., 1997) that implies the S_o values are larger than 0.42 nm^2. However, the close coincidence of experimental and calculated N_L and N_P values at $T > T_t$ as 245 and 2.26, respectively, indicates again on the conservation of particle radial dimensions at the DPPC phase transition.

Based on the data obtained in the present and previous (Dobretsov et al., 1998) study, the following model of lipid dynamics in apoA-I/DPPC complexes can be suggested (Fig. 7):

(a) At temperatures below T_t, *trans*-PA occupies the central lipid area with the radial dimensions from 0 to 3.8–4.3 nm (4.0 nm as a mean), while *cis*-PA is pushed to the disc periphery into the area with the dimensions from 1–2.5 nm (1.7 nm as a mean) to 5 nm. The lipid part of the rHDL particle can be divided then into three regions: (i) the zone I of weakly perturbed lipid lies between 0 and 1.7 nm with $S_o = 0.53$ nm^2 as the mean between 0.42 and 0.65 nm^2; (ii) the intermediate zone II between 1.7 and 4.0 nm with $S_o = 0.59$ nm^2 as the mean between the S_o values for zones I and III; (iii) the boundary lipid zone III between 4.0 and 5.0 nm with $S_o = 0.65$ nm^2. Then $N_L \approx 2\pi(1.7^2/0.53 + (4.0^2 - 1.7^2)/0.59 + 5.0^2 - 4.0^2)/0.65) \approx 260$; $N_P \approx N_L/(N_L/N_P) \approx 260/108 = 2.4$, that agrees well with the experimental data on rHDL composition. As S_o value seems to correlate reciprocally with the bilayer thickness H, then the unit area increase towards disc periphery results in the H decrease in this direction as much as 20%, i.e. at low temperatures the discoidal particles may possess the lens-like structure (Fig. 7a).

(b) At temperatures above T_t, it seems to be reasonable to assume: (1) the disappearance of the regional S_o variation with this parameter being fixed as 0.65 nm^2 and homogeneous localization of probe molecules in the bilayer; (2) the radius of lipid phase $R = 5.2$ nm, as follows from $2\pi R^2 = N_L S_o = 260 \cdot 0.65$ nm$^2 = 169$ nm^2; and (3) the localization of at least 50% of probe molecules in the region with the restricted probe mobility and close to the protein molecule. Then the next equation can be applied to estimate the radial size of this region as $(R - R_{rest})$:

$$\frac{\pi R^2 - \pi R_{rest}^2}{\pi R^2} \geq 0.5 \qquad (9)$$

and at $R = 5.2$ nm the relation exists $(R - R_{rest}) \geq 1.5$ nm as the lowest estimate for the boundary lipid region (Fig. 7b).

In summary, we conclude that the use of different partitioning of *cis*- and *trans*-isomers of parinaric acid between lipid regions with different lipid dynamics together with the ability of the probe to participate in the energy transfer from apolipoprotein tryptophan residues enabled us to

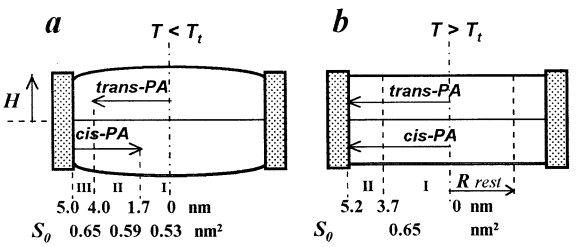

Fig. 7. The lipid regions with different dynamics in apoA-I/DPPC recombinants at $T < T_t$ (**a**) and at $T > T_t$ (**b**).

describe the molecular architecture of apoA-I/DPPC recombinants, the apolipoprotein localization and to characterize protein–lipid interactions at temperatures both below and above the phospholipid transition temperature. The existence of lipid regions with different lipid dynamics in apoA-I/DMPC recombinants had been previously reported (Tall and Lange, 1978; Massey et al., 1985). Protein–lipid interactions in the native plasma HDL particles is a key factor in the control of metabolism of these particles, in particular, their ability to accept cholesterol molecules. The structure of cholesterol-containing rHDL is currently under progress.

Acknowledgements

We are grateful to Dr M. Rosseneu (Laboratorium voor Lipoproteine Chemie/Vakgroep Biochemie, Universiteit Gent, Belgium) for allowing us to use the facilities in her laboratory and for a critical reading of our manuscript. Thanks are also due to Dr B. Vanloo who participated in the initial phase of the experiments. The excellent technical assistance of J. Taveirne and H. Caster is acknowledged. This work was supported by grant (98-04-48060) from the Russian Fond for Basic Reseach.

References

Bel'kov, M.N., Bondarev, S.L., Pavlenko, V.B., 1988. Spectral properties of retinyl acetate conformers in nonpolar solutions. Opt. Spectrosk. (Russia) 65, 1048–1052.

Birch, D.J.S., Birks, J.B., 1976. The photophysics of *trans*-stilbene. Chem. Phys. Lett. 38, 432–436.

Birch, D.J.S., Imhof, R.E., 1982. The origin of fluorescence from *trans*-*trans*-diphenylbutadiene. Chem. Phys. Lett. 88, 243–247.

Brasseur, R., Lins, L., Vanloo, B., Ruysschaert, J.-M., Rosseneu, M., 1992. Molecular modeling of the amphipathic helices of the plasma apolipoproteins. In: Proteins: Structure, Function and Genetics, vol. 13, pp. 246–257.

Christensen, R.L., Kohler, B.E., 1975. Vibronic coupling in polyenes: high resolution optical spectroscopy of 2,10-dimethylundecapentaene. J. Chem. Phys. 63, 1837–1846.

Christensen, R.L., Kohler, B.E., 1976. High-resolution optical spectroscopy of polyenes related to the visual chromophore. J. Phys. Chem. 80, 2197–2200.

Dergunov, A.D., Taveirne, J., Vanloo, B., Caster, H., Rosseneu, M., 1997. Structural organization of lipid phase and protein–lipid interface in apolipoprotein–phospholipid recombinants. Influence of cholesterol. Biochim. Biophys. Acta 1346, 131–146.

Dobretsov, G.E., Dergunov, A.D., Taveirne, J., Caster, H., Vanloo, B., Rosseneu, M., 1998. Apolipoprotein localization in reconstituted HDL particles: fluorescence energy transfer study. Chem. Phys. Lipids 97, 65–77.

Dobretsov, G.E., Kurek, N.K., Machov, V.N., Surejshchilova, T.I., Yakimenko, M.N., 1989. Determination of fluorescent probes localization in membranes by nonradiative energy transfer. J. Biochem. Biophys. Methods 19, 259–274.

Fielding, C.J., Fielding, P.E., 1995. Molecular physiology of reverse cholesterol transport. J. Lipid Res. 36, 211–228.

Gwynne, J., Brewer, B. Jr, Edelhoch, H., 1974. The molecular properties of apoA-I from human high density lipoprotein. J. Biol. Chem. 249, 2411–2416.

Jonas, A., 1986. Reconstitution of high-density lipoproteins. Meth. Enzymol. 128, 553–582.

Jonas, A., 1992. Lipid-binding properties of apolipoproteins. In: Rosseneu, M. (Ed.), Structure and Function of Apolipoproteins. CRC Press, Boca Raton, FL, pp. 217–250.

Jonas, A., Covinsky, K.E., Sweeny, S.A., 1985. Effects of amino group modification in discoidal apolipoprotein A-I-egg phosphatidylcholine–cholesterol complexes on their reactions with lecithin:cholesterol acyltransferase. Biochemistry 24, 3508–3513.

Jonas, A., Matz, C.E., 1982. Reaction of human lecithin:cholesterol acyltransferase with micellar substrates is independent of the phase state of the lipid. Biochemistry 21, 6867–6872.

Kimelman, D., Tecoma, E.S., Wolber, P.K., Hudson, B.S., Wickner, W.T., Simoni, R.D., 1979. Protein–lipid interactions. Studies of the M13 coat protein in dimyristoylphosphatidylcholine vesicles using parinaric acid. Biochemistry 18, 5874–5880.

Kurek, N.K., Lapshin, E.N., Dobretsov, G.E., Tur, I.N., Afanasiadi, L.S., 1989. 4-[-5-(Phenyloxazolil-20-1-pentadecyl] pyridinium-a fluorescent probe for determination of surface area of membranes and lipoproteins. Biol. Membr. (Russia) 6, 725–732.

Laemmli, U.K., 1970. Cleavage of structural proteins during the assembly of the head of bacteriophage T4. Nature 227, 680–685.

Lakowicz, J.R., 1983. Principles of Fluorescence Spectroscopy. Plenum Press, New York.

Lapshin, E.N., Dobretsov, G.E., Klebanov, G.I., Vladimirov, Y.A., 1983. Decondensing' effect of cholesterol on bilayers of the total egg phospholipids. Biophysics (Russia) 28, 752–755.

Levine, Y.K., 1972. Physical studies of membrane structure. Progr. Biophys. Mol. Biol. 24, 1–74.

Massey, J.B., She, H.S., Gotto, A.M. Jr, Pownall, H.J., 1985. Lateral distribution of phospholipid and cholesterol in

apolipoprotein A-I recombinants. Biochemistry 24, 7110–7116.

Owicki, J.C., McConnell, H.M., 1979. Theory of protein–lipid and protein–protein interactions in bilayer membranes. Proc. Natl. Acad. Sci. USA 76, 4750–4754.

Papahadjopoulos, D., Moscarello, M., Eylar, E.H., Isac, T., 1975. Effects of proteins on thermotropic phase transitions of phospholipid membranes. Biochim. Biophys. Acta 401, 317–335.

Pfanstiel, J.F., Champagne, B.B., Majewski, W.A., Plusquellic, D.F., Pratt, D.W., 1989. A rotationally resolved fluorescence excitation spectrum of all-trans-1,4-diphenyl-1,3-butadiene. Science 245, 736–738.

Phillips, M.C., 1972. The physical state of phospholipids and cholesterol in monolayers, bilayers and membranes. Progr. Surf. Membr. Sci. 5, 139–221.

Sklar, L., 1980. The partition of *cis*-parinaric acid and *trans*-parinaric acid among aqueous, fluid lipid, and solid lipid phases. Mol. Cell. Biochem. 32, 169–177.

Sklar, L.A., Hudson, B.S., Petersen, M., Diamond, J., 1977a. Conjugated polyene fatty acids as fluorescent probes: spectroscopic characterization. Biochemistry 16, 813–819.

Sklar, L.A., Hudson, B.S., Simoni, R.D., 1977b. Conjugated polyene fatty acids as fluorescent probes: synthetic phospholipid membrane studies. Biochemistry 16, 819–828.

Sklar, L.A., Miljanich, G.P., Dratz, E.A., 1979. Phospholipid phase separation and the partition of cis-parinaric acid and trans-parinaric acid among aqueous, solid lipid, and fluid lipid phases. Biochemistry 18, 1707–1716.

Sparks, D.L., Lund-Katz, S., Phillips, M.C., 1992a. The charge and structural stability of apolipoprotein A-I in discoidal and spherical recombinant high density lipoprotein particles. J. Biol. Chem. 267, 25839–25847.

Sparks, D.L., Phillips, M.C., Lund-Katz, S., 1992b. The conformation of apolipoprotein A-I in discoidal and spherical recombinant high density lipoprotein particles. J. Biol. Chem. 267, 25830–25838.

Tall, A.R., Lange, Y., 1978. Interaction of cholesterol, phospholipid and apoprotein in high density lipoprotein recombinants. Biochim. Biophys. Acta 513, 185–197.

Uphoff, R., Potthast, R., Dorfmuller, T., 1989. Reorientational motion of diphenylpolyenes in simple solvents as studied by depolarized light scattering and fluorescence anisotropy decay. J.Chem. Phys. 90, 6008–6017.

Van Tornout, P., Vercaemst, R., Lievens, M.J., Caster, H., Rosseneu, M., Assmann, G., 1980. Reassembly of human apoproteins A-I and A-II with unilamellar phosphatidylcholine–cholesterol liposomes. Association kinetics and characterization of the complexes. Biochim. Biophys. Acta 601, 509–523.

Waring, A.J., Glatz, P., Vanderkooi, J.M., 1979. Subzero temperature study of the inner mitochondrial membrane and related phospholipid membrane system with the fluorescent probe, trans-parinaric acid. Biochim. Biophys. Acta 557, 391–398.

Zhang, Y.-P., Lewis, R.N.A.H., Hodges, R.S., McElhaney, R.N., 1992. Interaction of a peptide model of a hydrophobic transmembrane α-helical segment of a membrane protein with phosphatidylcholine bilayers: differential scanning calorimetric and FTIR spectroscopic studies. Biochemistry 31, 11579–11588.